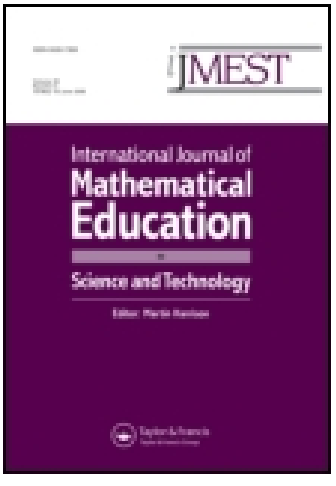

International Journal of Mathematical Education in Science and Technology
Publication details, including instructions for authors and subscription information:
http://www.tandfonline.com/loi/tmes20

A sacred geometry of the equilateral triangle

E.P. Doolan [a]
[a] Trinity College , Dublin, Republic of Ireland1
Published online: 18 Jun 2008.

To cite this article: E.P. Doolan (2008) A sacred geometry of the equilateral triangle, International Journal of Mathematical Education in Science and Technology, 39:5, 601-629, DOI: 10.1080/00207390701830164

To link to this article: http://dx.doi.org/10.1080/00207390701830164

International Journal of Mathematical Education in Science and Technology, Vol. 39, No. 5, 15 July 2008, 601–629

A sacred geometry of the equilateral triangle

E.P. Doolan*

Trinity College, Dublin, Republic of Ireland[1]

(*Received 8 May 2006*)

In this article, we investigate the construction of spirals on an equilateral triangle and prove that these spirals are geometric. In further analysing these spirals we show that both the male (straight line segments) and female (curves) forms of the spiral exhibit exactly the same growth ratios and that these growth ratios are constant independent of the iteration of the spiral. In particular, we show that ratio of any two successive radius vectors from the 'centre' of the spiral as we move inwards towards that 'centre' is always 1/2. This same elegant result is also shown to be true for successive chords. All our results are demonstrated using mostly coordinate and transformational geometry. Finally we look at two methods for constructing these spirals with ruler and compass to maximum accuracy.

Keywords: geometric spirals; equilateral triangle; sacred geometry; coordinate geometry; ruler and compass drawing

1. Binated equilateral triangles

1.1. *Introduction*

When geometric spirals (also called logarithmic or equiangular spirals) are mentioned, one generally thinks of the Fibonacci spiral constructed in a golden rectangle, whose long and short sides are in a ϕ relationship ($\phi =$ the golden proportion $= (1 + \sqrt{5})/2 = 1.6180339\ldots$) (Figure 1). Such geometric spirals can also be constructed in golden triangles [1].

However, geometric spirals can also be constructed using figures which do not have a ϕ relationship and this article discusses one such construction using an equilateral triangle.

As with the Fibonacci spiral we need to start by defining the process for successively creating the polygons on which the next portion of the spiral will be drawn. In our case this is a bination process on an equilateral triangle.

1.2. *The bination process*

The process of binating an equilateral triangle is achieved by joining the mid point of any side to the mid point of an opposite side. The new equilateral triangle so formed is called a binated (equilateral) triangle.

*Email: epdoolan@xs4all.nl
[1]Previous affiliation.

ISSN 0020–739X print/ISSN 1464–5211 online

DOI: 10.1080/00207390701830164
http://www.informaworld.com

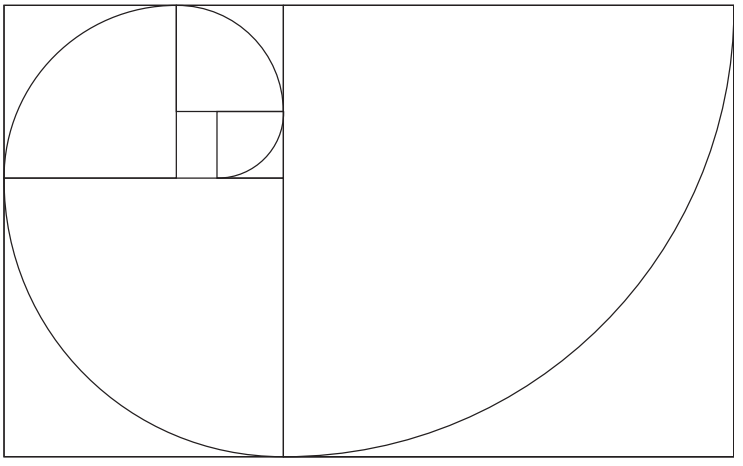

Figure 1. The geometric Fibonacci spiral in a golden rectangle.

Why is this a bination process? We know that the side of an equilateral triangle is $\sqrt{3}$ and that the height of an equilateral triangle is 3/2. When we join the mid points of opposite sides, the sides of the new triangle are $\sqrt{3}/2$ and the new height is 3/4 giving a new perimeter of $3\sqrt{3}/2$ and an area of $3\sqrt{3}/16$.

If we continue this process to the nth step then the side of the nth triangle is $\sqrt{3}/(2^n)$ and the height $3/2^{n+1}$, giving a perimeter of $3\sqrt{3}/(2^n)$ and area $3\sqrt{3}/(2^{2n+2})$, where $n=0$ for our basic triangle ΔABC.

In this way we see that for each successive step, the sides and height are half those of the previous triangle $(n-1)$. Furthermore, the perimeter is also halved and the area quartered. Thus, we can meaningfully talk of 'bination'.

1.3. *Bination patterns*

If we continue to binate each new binated triangle then there are in principle an infinite number of bination patterns within the original triangle. We will consider one particular pattern and look at the two variations of this which we do by defining, what we will choose to call, the (anti-) clockwise bination process.

We proceed as follows: Take an arbitrary equilateral triangle ΔABC and binate this triangle by bisecting the sides AB at D and AC at E. Join D and E.

Binate the resulting triangle ΔAED by bisecting the new line segment DE at G and the side AD at F. Join F and G. See Figure 2.

Continue this process by successively moving in a clockwise fashion and joining, for each new bination, the mid points of the newest line segment with the mid point of the adjacent side in anti-clockwise direction. The result of five clockwise binations of an equilateral triangle is shown in Figure 3.

In the above construction, we started with the vertex A by joining the mid points of the sides AB and AC. We could also have started with either of the two other vertices B or C, each of which would give a different pattern. Alternatively, this process can be done in a counter clockwise direction, starting with any one of the vertices A, B or C. The binated triangle is formed in this case by joining the mid point of the new side with the mid point of the adjacent side in *clockwise* direction. Thus binating successively in clockwise or

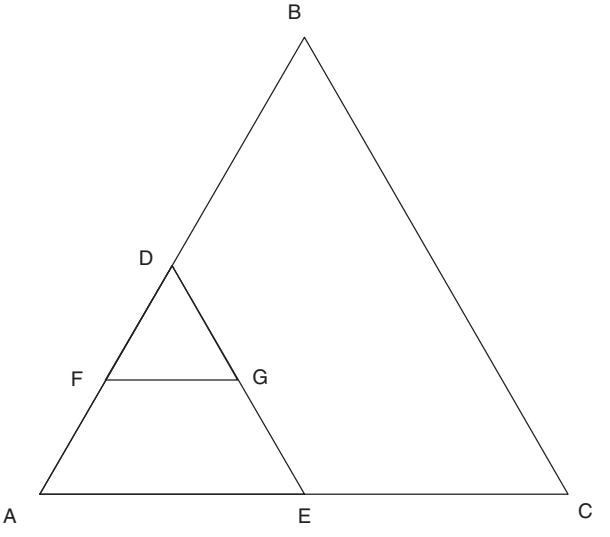

Figure 2. Two successive clockwise binations in an equilateral triangle with initial vertex A.

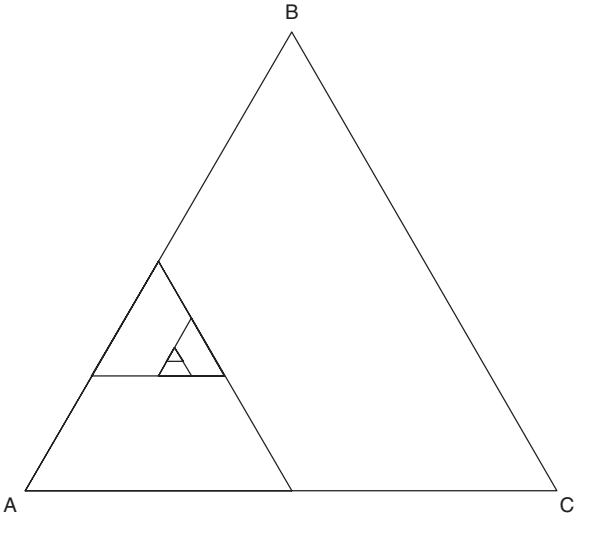

Figure 3. Five successive clockwise binations in an equilateral triangle with initial vertex A.

anti-clockwise direction leads to six possible bination patterns, three clockwise and three anti-clockwise. Three anti-clockwise bination patterns are shown in Figure 4.

We will now examine some properties of binated triangles. To assist in this we first derive the coordinates of our binated triangles.

1.4. *Coordinates of vertices of binated triangles*

In what follows we consider, without loss of generality, a standard triangle ΔABC whose bottom left hand corner (the vertex A) is situated at the origin (0, 0)

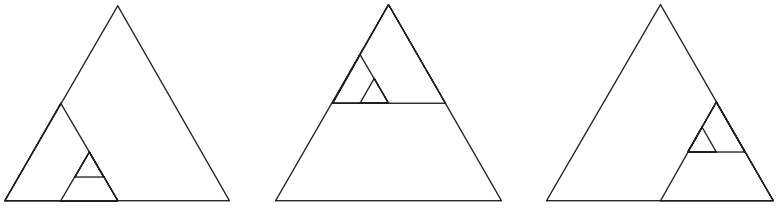

Figure 4. Successive anti-clockwise binated triangles for each vertex of an equilateral triangle.

and which has a circumradius of 1. The vertices B and C are then given by $(\sqrt{3}/2, 1/2)$ and $(\sqrt{3}, 0)$, respectively. Furthermore, we will always denote the vertex at the lower left hand corner of an equilateral triangle by A, the vertex at the top by B and the vertex at the lower right hand corner by C, independent of any rotations and/or reflections carried out.

In successive clockwise binations, the first bination with initial vertex A results in a binated triangle with a new side (DE in Figure 2) parallel to BC. Similarly, the second bination results in a new line segment parallel to AC (Figure 2) and the third in the new line segment parallel to AB. For the fourth bination, the process starts to repeat itself with a new line segment again parallel to BC, etc.

Thus, if n denotes the nth bination of the base triangle ΔABC corresponding to $n = 0$, we can write n as $n = 3m + \Theta$, with $n, m \geq 1$ and $\Theta = -2, -1$ or 0. We call m the *bination cycle* and Θ the *orientation*.

In Table 1, we give the coordinates of the vertices of the equilateral triangles resulting from three successive clockwise binations with initial vertex A. In this table, h is the height, s the length of a side and r the circumradius of the triangle in question.

To describe the coordinates of the general case we introduce the notation A_n^{dZ}, B_n^{dZ} and C_n^{dZ} for the vertices of the nth binated triangle where d denotes the direction (c for clockwise, a for anti-clockwise) and where Z denotes the initial vertex (A, B or C). We also introduce the commonly occurring quantity σ_m:

$$\sigma_m = \frac{\sum_{j=0}^{m-1} 2^{3j}}{2^{3m}} \tag{1}$$

for which we note the following identities that we will use repeatedly:

$$\sigma_m \equiv \frac{1}{8}(\sigma_{m-1} + 1) \tag{2}$$

and

$$\sigma_m \equiv \left(\sigma_{m-1} + \frac{1}{2^{3m}}\right). \tag{3}$$

These can be proved quite easily as follows:

$$\sigma_m = \frac{\sum_{j=0}^{m-1} 2^{3j}}{2^{3m}} = \frac{\left(\sum_{j=0}^{m-2} 2^{3j} + 2^{3(m-1)}\right)}{2^{3m-3} \cdot 2^3} = \frac{1}{8}\left(\frac{\sum_{j=0}^{m-2} 2^{3j}}{2^{3(m-1)}} + 1\right) = \frac{1}{8}(\sigma_{m-1} + 1)$$

and

$$\left(\sigma_{m-1} + \frac{1}{2^{3m}}\right) = \frac{\left(8\sum_{j=0}^{m-2} 2^{3j} + 1\right)}{2^{3m}} = \frac{\left(\sum_{j=0}^{m-2} 2^{3(j+1)} + 1\right)}{2^{3m}} = \frac{\left(\sum_{j=1}^{m-1} 2^{3j} + 2^0\right)}{2^{3m}} = \sigma_m$$

Table 1. The coordinates of three successive clockwise binated triangles with initial vertex A.

n	m	Θ	h	s	r	A_n^{cA}	B_n^{cA}	C_n^{cA}	Centre
0	–	–	$\frac{3}{2}$	$\sqrt{3}$	1	(0,0)	$\left(\frac{\sqrt{3}}{2}, \frac{3}{2}\right)$	$(\sqrt{3}, 0)$	$\left(\frac{\sqrt{3}}{2}, \frac{1}{2}\right)$
1	1	-2	$\frac{3}{4}$	$\frac{\sqrt{3}}{2}$	$\frac{1}{2}$	(0,0)	$\left(\frac{\sqrt{3}}{4}, \frac{3}{4}\right)$	$\left(\frac{\sqrt{3}}{2}, 0\right)$	$\left(\frac{\sqrt{3}}{4}, \frac{1}{4}\right)$
2	1	-1	$\frac{3}{8}$	$\frac{\sqrt{3}}{4}$	$\frac{1}{4}$	$\left(\frac{\sqrt{3}}{8}, \frac{3}{8}\right)$	$\left(\frac{\sqrt{3}}{4}, \frac{3}{4}\right)$	$\left(\frac{3\sqrt{3}}{8}, \frac{3}{8}\right)$	$\left(\frac{\sqrt{3}}{4}, \frac{1}{2}\right)$
3	1	0	$\frac{3}{16}$	$\frac{\sqrt{3}}{8}$	$\frac{1}{8}$	$\left(\frac{\sqrt{3}}{4}, \frac{3}{8}\right)$	$\left(\frac{5\sqrt{3}}{16}, \frac{9}{16}\right)$	$\left(\frac{3\sqrt{3}}{8}, \frac{3}{8}\right)$	$\left(\frac{5\sqrt{3}}{16}, \frac{7}{16}\right)$

Table 2. The coordinates of the vertices of the nth clockwise bination with initial vertex A.

Θ	$A_{3m+\Theta}^{cA}$	$B_{3m+\Theta}^{cA}$	$C_{3m+\Theta}^{cA}$	Length of side
-2	$(2\sqrt{3}(8\sigma_m - 1), 3(8\sigma_m - 1))$	$(2\sqrt{3}\sigma_m, 3(1 - 6\sigma_m))$	$(2\sqrt{3}(1 - 6\sigma_m), 3(8\sigma_m - 1))$	$4\sqrt{3}(1 - 7\sigma_m)$
-1	$(\sqrt{3}(9\sigma_m - 1), 3\sigma_m)$	$(2\sqrt{3}\sigma_m, 3(1 - 6\sigma_m))$	$(\sqrt{3}(1 - 5\sigma_m), 3\sigma_m)$	$2\sqrt{3}(1 - 7\sigma_m)$
0	$(2\sqrt{3}\sigma_m, 3\sigma_m)$	$\left(\frac{\sqrt{3}}{2}(1 - 3\sigma_m), \frac{3}{2}(1 - 5\sigma_m)\right)$	$\left(\sqrt{3}(1 - 5\sigma_m), 3\sigma_m\right)$	$\sqrt{3}(1 - 7\sigma_m)$

Furthermore, using the above identities, we have:

$$\sigma_m = \sigma_{m-1} + \frac{1}{2^{3m}} \Rightarrow \frac{1}{2^{3m}} = \sigma_m - \sigma_{m-1} = \frac{1}{8}(\sigma_{m-1} + 1) - \sigma_{m-1} = \frac{1}{8}(1 - 7\sigma_{m-1})$$

Hence, $\lim_{m\to\infty}(1 - 7\sigma_{m-1}) = \lim_{m\to\infty}(1/2^{3m-3}) = 0$, and therefore

$$\lim_{m\to\infty} \sigma_m = \frac{1}{7}. \tag{4}$$

Moreover, σ_m is a monotonically increasing sequence starting at 1/8 for $m = 1$ and approaching 1/7 as $m \to \infty$ so that $(1 - 7\sigma_m) \geq 0\ \forall m \geq 1$.

Another identity we will make regular use of is the following:

$$\left(\frac{1}{2^{3(m+1)}}\right)^2 \equiv \frac{1}{64}(1 - 7\sigma_m)^2 \tag{5}$$

which can be proved using both the identities (2) and (3).

Using Equations (1)–(3) we can now derive the coordinates of the vertices of the nth, $n \geq 1$, binated triangle in clockwise direction with initial vertex A for which $r = 1/2^{3m+\Theta} = 1/2^n$; $h = 3/(2 \cdot 2^{3\cdot m+\Theta}) = 3/2^{n+1}$; $s = \sqrt{3}/2^{3m+\Theta} = \sqrt{3}/2^n$.

To derive the coordinates of the other sets of triangles we begin by noting that the clockwise binated triangle coordinates with initial vertex B or C can be derived by simply rotating the vertices in Table 2 clockwise 120° and clockwise 240° (equivalent to −120°), respectively about the point $(\sqrt{3}/2,\ 1/2)$.

To rotate clockwise about an angle θ we need to remap the point of rotation $(\sqrt{3}/2,\ 1/2)$ to the origin (0, 0), multiply the resulting coordinates by the matrix

$\begin{pmatrix} \cos\theta & \sin\theta \\ -\sin\theta & \cos\theta \end{pmatrix}$ and translate the origin back to its original location. Rotating the vertex A_{3m}^{cA} for example through 120° and naming the vertices as before, we get the following:

$$\begin{pmatrix} -\frac{1}{2} & \frac{\sqrt{3}}{2} \\ -\frac{\sqrt{3}}{2} & -\frac{1}{2} \end{pmatrix} \begin{pmatrix} \sqrt{3}\left(2\sigma_m - \frac{1}{2}\right) \\ \left(3\sigma_m - \frac{1}{2}\right) \end{pmatrix} = \left(\frac{\sqrt{3}}{2}\sigma_m, 1 - \frac{9\sigma_m}{2}\right)$$

and translating the origin back to its original location we get:

$$B_{3m}^{cB} = \left(\frac{\sqrt{3}}{2}(1+\sigma_m),\ \frac{3}{2}(1-3\sigma_m)\right).$$

Tables 3 and 4 show the results of completing the rotations for the other vertices.

To derive the anti-clockwise coordinates we note that reflecting the set of clockwise binated triangles with initial vertex A through the median $y = -(1/\sqrt{3})x + 1$ gives the set of anti-clockwise binated triangles with initial vertex B (Figure 5).

Reflecting vertices in the line $y = -(1/\sqrt{3})x + 1$ is equivalent to rotating them through $-30°$ after moving the origin to $(\sqrt{3}, 0)$, reflecting the result in the y axis (changing the sign of the y coordinate), rotating back through 30° and finally translating the origin back to its original position. Reflecting the vertex A_{3m}^{cA} for example in the median $y = -(1/\sqrt{3})x + 1$ and naming the vertices as before, gives the following:

Remapping the origin and rotating through −30°:

$$\begin{pmatrix} \frac{\sqrt{3}}{2} & -\frac{1}{2} \\ \frac{1}{2} & \frac{\sqrt{3}}{2} \end{pmatrix} \begin{pmatrix} \sqrt{3}(2\sigma_m - 1) \\ 3\sigma_m \end{pmatrix} = \left(\frac{3}{2}(\sigma_m - 1), \frac{\sqrt{3}}{2}(5\sigma_m - 1)\right).$$

Reflecting in the y-axis gives:

$$\left(\frac{3}{2}(\sigma_m - 1), \frac{\sqrt{3}}{2}(1 - 5\sigma_m)\right).$$

Rotating back though 30°:

$$\begin{pmatrix} \frac{\sqrt{3}}{2} & \frac{1}{2} \\ -\frac{1}{2} & \frac{\sqrt{3}}{2} \end{pmatrix} \begin{pmatrix} \frac{3}{2}(\sigma_m - 1) \\ \frac{\sqrt{3}}{2}(1 - 5\sigma_m) \end{pmatrix} = \left(-\frac{\sqrt{3}}{2}(1+\sigma_m), \frac{3}{2}(1-3\sigma_m)\right)$$

and translating the origin back to its original location gives

$$B_{3m}^{aB} = \left(\frac{\sqrt{3}}{2}(1-\sigma_m), \frac{3}{2}(1-3\sigma_m)\right).$$

Completing the reflections for the other vertices gives Table 5.

Similarly, rotating these vertices through 120° and 240° as before for the clockwise vertices gives the coordinates of the anti-clockwise binated triangles with initial vertices C and A, respectively.

Table 3. The coordinates of clockwise binated triangles with initial vertex B.

Θ	$A^{cB}_{3m+\Theta}$	$B^{cB}_{3m+\Theta}$	$C^{cB}_{3m+\Theta}$
-2	$\left(2\sqrt{3}(9\sigma_m - 1), 6\sigma_m\right)$	$\left(4\sqrt{3}\sigma_m, 6(1 - 6\sigma_m)\right)$	$\left(2\sqrt{3}(1 - 5\sigma_m), 6\sigma_m\right)$
-1	$\left(4\sqrt{3}\sigma_m, 6\sigma_m\right)$	$\left(\sqrt{3}(1 - 3\sigma_m), 3(1 - 5\sigma_m)\right)$	$\left(2\sqrt{3}(1 - 5\sigma_m), 6\sigma_m\right)$
0	$\left(4\sqrt{3}\sigma_m, 6\sigma_m\right)$	$\left(\frac{\sqrt{3}}{2}(1 + \sigma_m), \frac{3}{2}(1 - 3\sigma_m)\right)$	$\left(\sqrt{3}(1 - 3\sigma_m), 6\sigma_m\right)$

Table 4. The coordinates of clockwise binated triangles with initial vertex C.

Θ	$A^{cC}_{3m+\Theta}$	$B^{cC}_{3m+\Theta}$	$C^{cC}_{3m+\Theta}$
-2	$\left(\frac{\sqrt{3}}{2}(16\sigma_m - 1), \frac{3}{2}(8\sigma_m - 1)\right)$	$\left(\frac{3\sqrt{3}}{2}(1 - 4\sigma_m), \frac{3}{2}(3 - 20\sigma_m)\right)$	$\left(\frac{\sqrt{3}}{2}(7 - 40\sigma_m), \frac{3}{2}(8\sigma_m - 1)\right)$
-1	$\left(\frac{\sqrt{3}}{2}(16\sigma_m - 1), \frac{3}{2}(8\sigma_m - 1)\right)$	$\left(\frac{\sqrt{3}}{2}(2\sigma_m + 1), \frac{3}{2}(1 - 6\sigma_m)\right)$	$\left(\frac{3\sqrt{3}}{2}(1 - 4\sigma_m), \frac{3}{2}(8\sigma_m - 1)\right)$
0	$\left(\frac{9\sqrt{3}}{2}\sigma_m, \frac{3}{2}\sigma_m\right)$	$\left(\frac{\sqrt{3}}{2}(2\sigma_m + 1), \frac{3}{2}(1 - 6\sigma_m)\right)$	$\left(\frac{\sqrt{3}}{2}(2 - 5\sigma_m), \frac{3}{2}\sigma_m\right)$

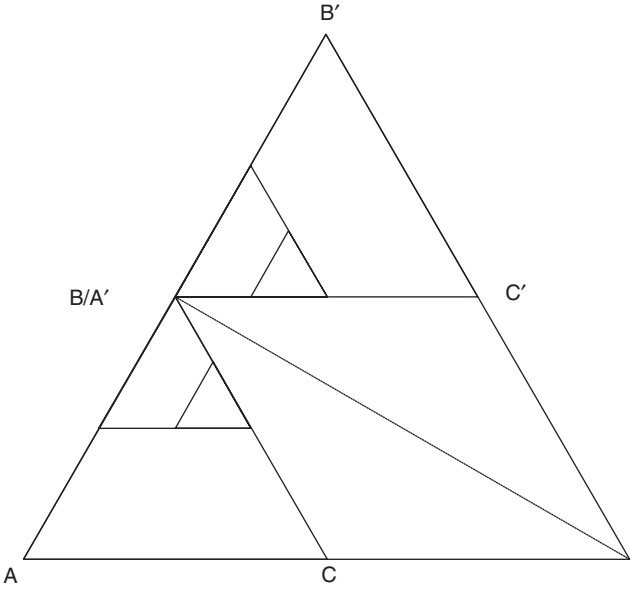

Figure 5. Using reflection through a median to produce an anti-clockwise binated triangle with initial vertex B.

Table 5. The coordinates of anti-clockwise binated triangles with initial vertex B.

Θ	$A^{aB}_{3m+\Theta}$	$B^{aB}_{3m+\Theta}$	$C^{aB}_{3m+\Theta}$
-2	$\left(\sqrt{3}(10\sigma_m - 1), 6\sigma_m\right)$	$\left(\sqrt{3}(1 - 4\sigma_m), 6(1 - 6\sigma_m)\right)$	$\left(3\sqrt{3}(1 - 6\sigma_m), 6\sigma_m\right)$
-1	$\left(\sqrt{3}(10\sigma_m - 1), 6\sigma_m\right)$	$\left(3\sqrt{3}\sigma_m, 3(1 - 5\sigma_m)\right)$	$\left(\sqrt{3}(1 - 4\sigma_m), 6\sigma_m\right)$
0	$\left(3\sqrt{3}\sigma_m, 6\sigma_m\right)$	$\left(\frac{\sqrt{3}}{2}(1 - \sigma_m), \frac{3}{2}(1 - 3\sigma_m)\right)$	$\left(\sqrt{3}(1 - 4\sigma_m), 6\sigma_m\right)$

1.5. *Properties of binated triangles*

We will now show that all the corresponding vertices of triangles with the same orientation are collinear. In other words, all the vertices A^{dZ}_n, B^{dZ}_n and C^{dZ}_n where $n = 3m + \Theta$ for a fixed Θ, initial vertex Z and fixed direction d, are collinear.

Theorem 1: *For a fixed orientation Θ and initial vertex Z, all the corresponding vertices $Y^{dZ}_{3m+\Theta}$ of binated triangles with a fixed direction d lie on a straight line $\forall\ m \geq 1$ and $Y = A$, B or C.*

Proof: We will only prove this for one set of vertices for one direction, one orientation and one initial vertex A; the proof for the other vertices being analogous.

Take the set of vertices C^{cA}_n, where $n = 3m - 2$, n, $m \geq 1$, $\Theta = -2$, $d = c$ and $Z = A$.

Using Table 2, the slope $s = (y_2 - y_1)/(x_2 - x_1)$ of the line through $C^{cA}_{3(m-1)-2}$ and C^{cA}_{3m-2} is given by:

$$s = \frac{(24\sigma_m - 3 - 24\sigma_{m-1} + 3)}{\left(2\sqrt{3} - 12\sqrt{3}\sigma_m - 2\sqrt{3} + 12\sigma_{m-1}\right)} = \frac{-2}{\sqrt{3}}.$$

Similarly the slope s' of the line through $C^{cA}_{3(m-1)-2}$ and $C^{cA}_{3(m+1)-2}$ is given by:

$$s' = \frac{(24\sigma_{m+1} - 3 - 24\sigma_{m-1} + 3)}{\left(2\sqrt{3} - 12\sqrt{3}\sigma_{m+1} - 2\sqrt{3} + 12\sigma_{m-1}\right)} = \frac{-2}{\sqrt{3}}.$$

Therefore, since the slopes of lines joining $C^{cA}_{3(m-1)-2}$ with C^{cA}_{3m-2} and with $C^{cA}_{3(m+1)-2}$ are the same, these three points must be collinear and we conclude that the set of vertices C^{cA}_n, where $n = 3m - 2$, n, $m \geq 1$, all lie on the same straight line, which completes the proof. □

We introduce the notation $\bar{A}^{dZ}_n, \bar{B}^{dZ}_n$ and $\bar{C}^{dZ}_n$ to denote the lines through a set of vertices with the same direction d, orientation Θ and initial vertex Z. Figure 6 shows one set of these lines for $\Theta = -1$.

Theorem 2: *For a given direction d and a given initial vertex Z, the 9 lines $\bar{Y}^{dZ}_{3m+\Theta}$ joining the vertices of successive binations for the three different orientations Θ of an equilateral triangle meet at a point.*

Proof: We will only prove this for clockwise binated triangles with initial vertex A ($d = c$, $Z = A$).

We first compute, as illustrated in Theorem 1 using Table 2, the slopes of the lines $\bar{A}^{cA}_{3m-2}, \bar{B}^{cA}_{3m-2}, \bar{C}^{cA}_{3m-2}$; these are $\sqrt{3}/2$, $-3\sqrt{3}$ and $-2/\sqrt{3}$ respectively. Now using Table 2

again for the coordinates of the vertices $A^{cA}_{3m-2}, B^{cA}_{3m-2}$ and C^{cA}_{3m-2} we compute the absissae of the lines $y = mx + c$ as follows:

$\bar{A}^{cA}_{3m-2} : y = (\sqrt{3}/2)x + c$ and this line passes through the point $(2\sqrt{3}(8\sigma_m - 1), 3(8\sigma_m - 1))$, which gives $c = 0$.
$\bar{B}^{cA}_{3m-2} : y = -3\sqrt{3}x + c$ and this line passes through the point $(2\sqrt{3}\sigma_m, 3(1 - 6\sigma_m))$, which gives $c = 3$.
$\bar{C}^{cA}_{3m-2} : y = (-2/\sqrt{3})x + c$ and this line passes through the point $(2\sqrt{3}(1 - 6\sigma_m), 3(8\sigma_m - 1))$, which gives $c = 1$.

The intersection of the lines $\bar{A}^{cA}_{3m-2}$ and $\bar{B}^{cA}_{3m-2}$ is at the point $(2\sqrt{3}/7, 3/7)$ and it can seen that this point also lies on the line $\bar{C}^{cA}_{3m-2}$. Therefore, the three lines $\bar{A}^{cA}_{3m-2}$, $\bar{B}^{cA}_{3m-2}$ and $\bar{C}^{cA}_{3m-2}$ meet at a common point.

An exact analogous proof shows that the three lines $\bar{A}^{cA}_{3m-1}, \bar{B}^{cA}_{3m-1}$ and $\bar{C}^{cA}_{3m-1}$ meet at the common point $(2\sqrt{3}/7, 3/7)$ as do the three lines $\bar{A}^{cA}_{3m}, \bar{B}^{cA}_{3m}$ and $\bar{C}^{cA}_{3m}$. This completes the proof. □

We now introduce the notation $Z^d_\bullet$ to denote the common point at which the lines $\bar{A}^{dZ}_n, \bar{B}^{dZ}_n$ and $\bar{C}^{dZ}_n$ intersect and we call the point $Z^d_\bullet$ a *convergence point*. Table 6 gives the six convergence points for clockwise and anti-clockwise binated triangles.

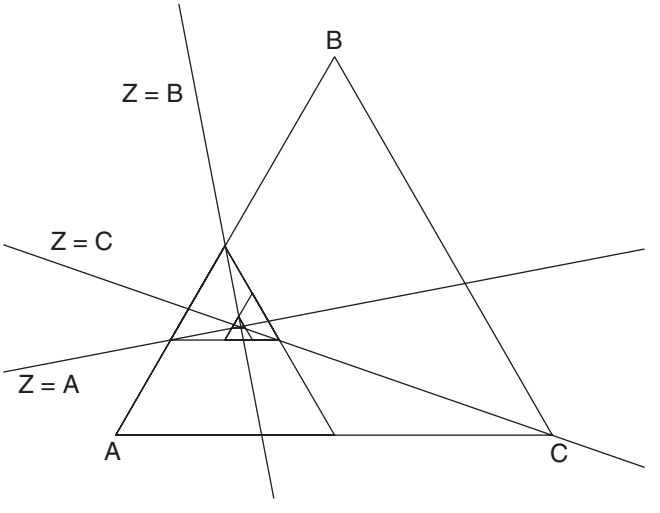

Figure 6. The lines $\bar{Z}^{cA}_{3m-1}$ through the vertices of clockwise binated triangles with initial vertex A.

Table 6. The coordinates $Z^d_\bullet$ of the clockwise and anti-clockwise convergence points.

	$A^d_\bullet$	$B^d_\bullet$	$C^d_\bullet$
Clockwise	$\left(\frac{2\sqrt{3}}{7}, \frac{3}{7}\right)$	$\left(\frac{4\sqrt{3}}{7}, \frac{6}{7}\right)$	$\left(\frac{9\sqrt{3}}{14}, \frac{3}{14}\right)$
Anti-clockwise	$\left(\frac{5\sqrt{3}}{14}, \frac{3}{14}\right)$	$\left(\frac{3\sqrt{3}}{7}, \frac{6}{7}\right)$	$\left(\frac{5\sqrt{3}}{7}, \frac{3}{7}\right)$

By continuously binating triangles we get a series of spiralling triangles which become smaller and smaller. Ultimately these triangles converge to a single point, the convergence point just introduced. This can be seen by taking the $\lim_{m\to\infty}\sigma_m$ (Equation (4)) of the vertices of the binated triangles as given, for example, in Tables 2–5.

1.6. *Convergence triangles*

We call the triangles defined by the three points $A^d_\bullet, B^d_\bullet$ and $C^d_\bullet$ for a fixed direction clockwise or anti-clockwise *convergence triangles*, respectively. We now note some properties of convergence triangles.

Theorem 3: *The triangles formed by the convergence points* $A^d_\bullet, B^d_\bullet$ *and* $C^d_\bullet$ *for the clockwise or anti-clockwise binated triangles are equilateral triangles with the same circumcentre* $(\sqrt{3}/2, 1/2)$ *as the original triangle and with circumradius* $1/\sqrt{7}$.

Proof: We look at the clockwise convergence triangle only. An analogous proof follows for the anti-clockwise convergence triangle.

Using the formula $\sqrt{(x_1-x_2)^2+(y_1-y_2)^2}$ for the distance between two points $(x_1, y_1)\,\&\,(x_2, y_2)$ and Table 6, the length of any of the sides $A^c_\bullet B^c_\bullet, B^c_\bullet C^c_\bullet, C^c_\bullet A^c_\bullet$ is seen to be $\sqrt{3/7}$. $\therefore$ The triangle $\Delta A^c_\bullet B^c_\bullet C^c_\bullet$ is an equilateral triangle.

The circumcentre of an equilateral triangle is given by the intersection of the lines joining the mid points of the sides to the opposite vertex. For the clockwise convergence triangle:
The median joining the mid point $(3\sqrt{3}/7, 9/14)$ of $A^c_\bullet B^c_\bullet$ and the vertex $C^c_\bullet$ is $y = -(2/\sqrt{3})x + (3/2)$, which is actually the line $\bar{C}^{cC}_{3m-1}$ as computed in Theorem 2.
The median joining the mid point $(17\sqrt{3}/28, 15/28)$ of $B^c_\bullet C^c_\bullet$ and the vertex $A^c_\bullet$ is $y = (1/3\sqrt{3})x + (1/3)$, which is actually the line $\bar{A}^{cA}_{3m-1}$.
This is illustrated in Figure 7, which builds on Figure 6.

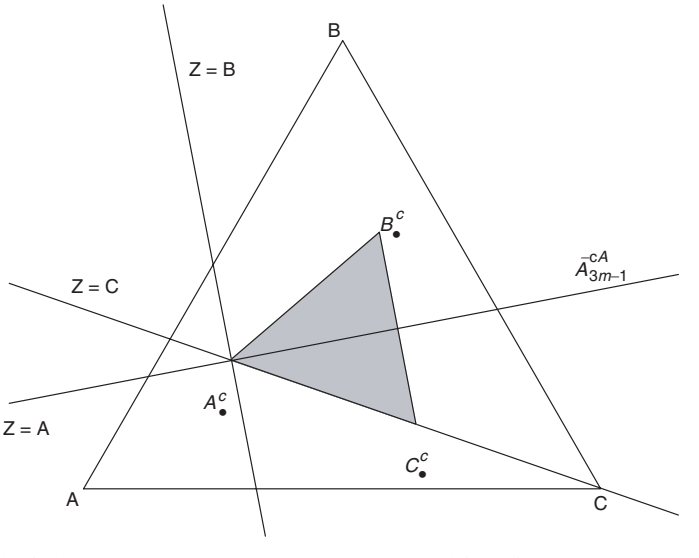

Figure 7. The clockwise convergence triangle $\Delta A^c_\bullet B^c_\bullet C^c_\bullet$ within the triangle ΔABC, showing the median $\bar{A}^{cA}_{3m-1}$.

The intersection of these two lines is at $(\sqrt{3}/2, 1/2)$, which is the circumcentre of the original triangle ΔABC.

Finally, the distance from the circumcentre to any vertex of the clockwise convergence triangle is seen to be $1/\sqrt{7}$. This completes the proof. □

The convergence triangles are a factor $1/\sqrt{7}$ smaller (side, circumradius, height) than the original triangle and are rotated clockwise or anti-clockwise about the circumcentre of the original triangle ΔABC. The angle of rotation is computed as follows:

We have just seen that the equation of line joining the mid point $(3\sqrt{3}/7, 9/14)$ of $A^c_\bullet B^c_\bullet$ and the vertex $C^c_\bullet$ is given by:

$$y = -\frac{2}{\sqrt{3}}x + \frac{3}{2}.$$

Similarly the equation of the line through the mid point $(\sqrt{3}/4, 3/4)$ of AB and the vertex C is given by:

$$y = -\frac{1}{\sqrt{3}}x + 1.$$

Using the formula for the angle between two lines of slopes m_1 and m_2, arc $\tan((m_1 - m_2)/1 + m_1 m_2)$, we see that $\Delta A^c_\bullet B^c_\bullet C^c_\bullet$ is rotated by arc $\tan(\sqrt{3}/5)$, or approximately 19.1°, in a clockwise direction with respect to ΔABC.

Similarly the anti-clockwise convergence triangle $\Delta A^a_\bullet B^a_\bullet C^a_\bullet$ is rotated by approximately 19.1° in an anti-clockwise direction with respect to ΔABC.

The fact that the angle arc $\tan(\sqrt{3}/5)$ is transcendental means that if we continue the process of bination by successively binating each resulting convergence triangle, no two convergence triangles ever have exactly the same orientation in space.

2. Equilateral spirals

We are now in a position to define our spirals which we will call *equilateral spirals*. We start with the male spiral, which is constructed from straight line segments.

2.1. *The male equilateral spiral*

In Section 1.3, we have seen that when we binate an equilateral triangle, the new binated triangle has two sides which overlap with the sides of the existing equilateral triangle and one new side. In Figure 2, for example, the side DE is the new side. We now define a segment of the male equilateral spiral as being that side of triangle which is left (anti-clockwise) for a clockwise binated triangle and right (clockwise) for an anti-clockwise binated triangle of the new side of the binated triangle in question. Since the bination process also always bisects the new side created in the previous bination, it follows that the segments of the male spiral so defined form a continuous set of straight line segments.

Seven segments of a male clockwise spiral with initial vertex A are shown in Figure 8.

2.2. *The female equilateral spiral*

The female equilateral spiral also uses the binated triangles as its basis. In this case, instead of simply using the side of triangle to the left or right of the newest side for a female spiral,

we construct the arc of the circumcircle of that triangle on that side. The centre of the circumcircle is, as we know, given by the intersection of the medians (lines joining the mid points of the sides to the opposite vertices) and that they meet in a point. The female equilateral spiral is formed by constructing the successive circumcircle arcs on the corresponding line segments of the male equilateral spiral. Since the male spiral is formed by a continuous set of straight line segments, it follows that the female equilateral spiral is also a continuous curve.

To be able to construct the arc segments we need to compute the centres of the binated triangles. For the circumcentre of the nth binated triangle we introduce the notation Δ_n^{dZ}, where d is the direction and Z, the initial vertex. The x coordinate of the centre is given by the x coordinate of the vertex B_n^{dZ} at the top of the triangle. Since the medians trisect each other, we need for the y coordinate of the circumcentre only to add one third of the height to y coordinate of A_n^{dZ} or C_n^{dZ}. For example, for the y coordinate of the nth clockwise binated triangle ($\Theta = -2$, $n = 3m - 2$) with initial vertex A we have, using Table 2:

$$y_n = 3(8\sigma_m - 1) + \frac{1}{3}(3(1 - 6\sigma_m) - 3(8\sigma_m - 1)) = 3(8\sigma_m - 1) + (2 - 14\sigma_m) = 10\sigma_m - 1$$

We obtain Table 7 by completing the computations for the centres of the other clockwise-binated triangles.

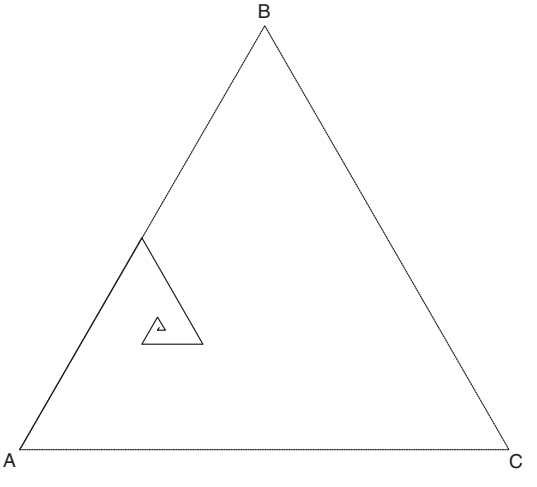

Figure 8. Seven segments of a male clockwise equilateral spiral with initial vertex A.

Table 7. The coordinates of the centres of clockwise-binated triangles.

Θ	Centre $\Delta_{3m+\Theta}^{cA}$	Centre $\Delta_{3m+\Theta}^{cB}$	Centre $\Delta_{3m+\Theta}^{cC}$
-2	$\left(2\sqrt{3}\sigma_m, (10\sigma_m - 1)\right)$	$\left(4\sqrt{3}\sigma_m,\ 2(1 - 4\sigma_m)\right)$	$\left(\frac{3\sqrt{3}}{2}(1 - 4\sigma_m),\ \frac{1}{2}(1 - 4\sigma_m)\right)$
-1	$\left(2\sqrt{3}\sigma_m,\ 1 - 4\sigma_m\right)$	$\left(\sqrt{3}(1 - 3\sigma_m),\ (1 - \sigma_m)\right)$	$\left(\frac{\sqrt{3}}{2}(2\sigma_m + 1),\ \frac{1}{2}(10\sigma_m - 1)\right)$
0	$\left(\frac{\sqrt{3}}{2}(1 - 3\sigma_m),\ \frac{1}{2}(1 - \sigma_m)\right)$	$\left(\frac{\sqrt{3}}{2}(1 + \sigma_m),\ \frac{1}{2}(1 + 5\sigma_m)\right)$	$\left(\frac{\sqrt{3}}{2}(2\sigma_m + 1),\ \frac{1}{2}(1 - 4\sigma_m)\right)$

For the circumcentres Δ_n^{dZ} we note the following two properties:

- The triangles $\triangle \Delta_n^{dA}\Delta_n^{dB}\Delta_n^{dC}$ for a fixed n and a fixed direction d, are equilateral triangles. This can be seen by simply computing the lengths of the sides using Pythagoras.
- The triangles $\triangle \Delta_{3m-2}^{dZ}\Delta_{3m-1}^{dZ}\Delta_{3m}^{dZ}$ for a fixed direction d and an initial vertex Z, are right angled triangles. Again using Pythagoras, we see that the lengths of the sides in this case are $(1-7\sigma_m)$, $\sqrt{3}(1-7\sigma_m)$ and $2(1-7\sigma_m)$ $(=\sqrt{(1-7\sigma_m)^2+(\sqrt{3}(1-7\sigma_m))^2})$, respectively.

Figure 9 shows the clockwise equilateral spiral with initial vertex A made up of seven successive arc segments.

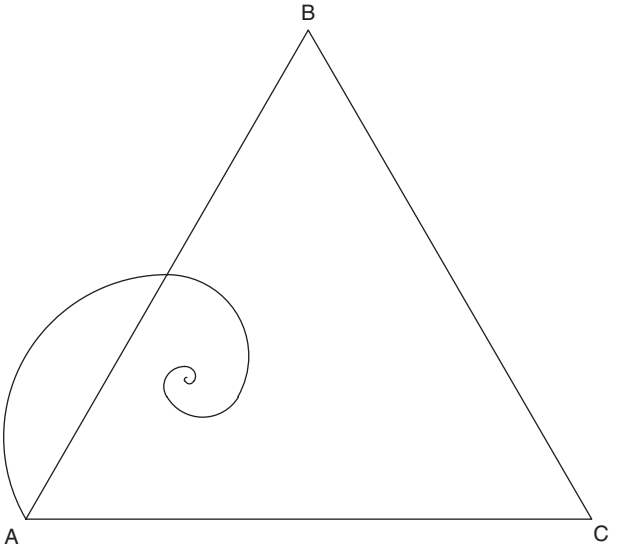

Figure 9. Seven segments of a female clockwise equilateral spiral with initial vertex A.

We will now show that these female equilateral spirals are smooth.

Theorem 4: *Equilateral female spirals are C^1 continuous.*

Proof: We will only prove this for clockwise spirals, the proof for anti-clockwise spirals being completely analogous.

Since the constituent segments of any spiral are arcs of circles and since circles are C^1 so are the arcs between the two end points. Thus we only need to look at the points where these arc segments actually connect to each other.

Since by construction (see Sections 2.1 and 2.2) successive arcs form a continuous curve and are thus C^0, we will now look at the continuity of the first derivative of the functions defined by the arcs at the points at which these arcs meet.

We will do this by looking at the derivatives of the functions defining the arcs and evaluating these derivatives at the points of connection as we come from the right and the left to that point of connection. We will show that the derivatives of the functions defining the arcs and evaluated at the points of connection are in fact independent of σ_m.

For an initial vertex A, the generic points at which successive arc segments of a female equilateral clockwise spiral are connected are:

$A^{cA}_{3(m-1)}\left(\text{centre } \Delta^{dA}_{3(m-1)}\right)$ and $A^{cA}_{3m-2}\left(\text{centre } \Delta^{dA}_{3m-2}\right)$, $B^{cA}_{3m-2}\left(\text{centre } \Delta^{dA}_{3m-2}\right)$ and $B^{cA}_{3m-1}\left(\text{centre } \Delta^{dA}_{3m-1}\right)$, $C^{cA}_{3m-1}\left(\text{centre } \Delta^{dA}_{3m-1}\right)$ and $C^{cA}_{3m}\left(\text{centre } \Delta^{dA}_{3m}\right)$ and $A^{cA}_{3m}\left(\text{centre } \Delta^{dA}_{3m}\right)$ and $A^{cA}_{3(m+1)-2}\left(\text{centre } \Delta^{dA}_{3(m+1)-2}\right)$.

The equation of a circle with centre (a, b) and radius r is:

$$(x-a)^2+(y-b)^2=r^2 \text{ with the first derivative being } \frac{\mathrm{d}y}{\mathrm{d}x}=\frac{a-x}{y-b}.$$

Using Tables 2 and 7 to compute the first derivative of the equations of the circles with centres as indicated above and evaluating these derivatives at the corresponding connection points, we get:

$$A^{cA}_{3(m-1)}: \quad \frac{\mathrm{d}y}{\mathrm{d}x}=\frac{(\sqrt{3}/2)(1-3\sigma_{m-1})-2\sqrt{3}\sigma_{m-1}}{3\sigma_{m-1}-(1/2)(1-\sigma_{m-1})}=-\sqrt{3}$$

$$A^{cA}_{3m-2}: \quad \frac{\mathrm{d}y}{\mathrm{d}x}=\frac{2\sqrt{3}\sigma_m-2\sqrt{3}(8\sigma_m-1)}{3(8\sigma_m-1)-(10\sigma_m-1)}=-\sqrt{3}$$

$$B^{cA}_{3m-2}: \quad \frac{\mathrm{d}y}{\mathrm{d}x}=\frac{2\sqrt{3}\sigma_m-2\sqrt{3}\sigma_m}{3(1-6\sigma_m)-(10\sigma_m-1)}=0$$

$$B^{cA}_{3m-1}: \quad \frac{\mathrm{d}y}{\mathrm{d}x}=\frac{2\sqrt{3}\sigma_m-2\sqrt{3}\sigma_m}{3(1-6\sigma_m)-(1-4\sigma_m)}=0$$

$$C^{cA}_{3m-1}: \quad \frac{\mathrm{d}y}{\mathrm{d}x}=\frac{2\sqrt{3}\sigma_m-\sqrt{3}(1-5\sigma_m)}{3\sigma_m-(1-4\sigma_m)}=\sqrt{3}$$

$$C^{cA}_{3m}: \quad \frac{\mathrm{d}y}{\mathrm{d}x}=\frac{(\sqrt{3}/2)(1-3\sigma_m)-\sqrt{3}(1-5\sigma_m)}{3\sigma_m-(1/2)(1-\sigma_m)}=\sqrt{3}$$

and since all these derivatives, and in particular those evaluated at $A^{cA}_{3(m-1)}$ and A^{cA}_{3m-2}, are constants independent of σ_m, we can conclude that the first derivatives evaluated at A^{cA}_{3m} and $A^{cA}_{3(m+1)-2}$ are also equal. This completes the proof. □

One of the essential properties of a geometric spiral is that if we draw a line from any point on the spiral to the centre (the convergence point), then the angle this line makes to the tangents at all the points at which it cuts the spiral are the same. A geometric spiral is thus a shape that remains the same regardless of size. We will now show that both the male and female spirals we have defined are indeed geometric spirals.

Theorem 5: *Equilateral female spirals are geometric spirals, i.e. the tangents at the intersection points formed by any line drawn through the spiral and which also passes through the convergence point* (*we call such lines radius vectors*), *are at a constant angle to the radius vector*.

Proof: We will only prove this for the clockwise spiral with initial vertex A, the proof for all other equilateral spirals within the triangle being completely analogous.

The mth *iteration* of a clockwise female equilateral spiral with initial vertex A consists of three segments of arc length $2\pi/3$ as follows:

(a) Segment $3m-2$, an arc of the circle with centre Δ^{dA}_{3m-2} which runs from A^{cA}_{3m-2} to B^{cA}_{3m-2}.
(b) Segment $3m-1$, an arc of the circle with centre Δ^{dA}_{3m-1} which runs from B^{cA}_{3m-1} to C^{cA}_{3m-1}.
(c) Segment $3m$, an arc of the circle with centre Δ^{dA}_{3m} which runs from C^{cA}_{3m} to A^{cA}_{3m}.

- The vertices $Y^{cA}_{3m+\Theta}$ are specified in Table 2.
- The centres of the circles, $\Delta^{dA}_{3m+\Theta}$, from which the arc segments of the spiral are drawn are given in Table 7.
- The convergence point for clockwise spiral with initial vertex A is given in Table 6.

We will now look at the segments $3m-2$, $3m-1$ and $3m$ and show that the angle the tangent at any point (x, y) on the segment makes with the radius vector joining this point to the convergence point is a constant independent of σ_m, and thus also of m.

Segment $3m-2$

The slope of the radius vector from any point (x, y) on the circle with centre Δ^{dA}_{3m-2} to the convergence point $A^{c}_{\bullet}$ is given by:

$$m_1 = \frac{(y-(3/7))}{\left(x-\left(2\sqrt{3}/7\right)\right)} \tag{6}$$

The slope of the tangent at any point (x, y) on any circle with centre Δ^{dA}_{3m-2} is given by:

$$m_2 = \frac{-\left(x-2\sqrt{3}\sigma_m\right)}{(y-(10\sigma_m-1))}$$

The angle between the tangent and the radius vector is given by:

$$\text{arc tan}\left(\frac{m_1-m_2}{1+m_1m_2}\right).$$

We will now show that the argument to the arc tan function is independent of σ_m:

$$\frac{m_1-m_2}{1+m_1m_2} = \frac{(y-3/7)(y-(10\sigma_m-1))+\left(x-2\sqrt{3}\sigma_m\right)\left(x-2\sqrt{3}/7\right)}{\left(x-2\sqrt{3}/7\right)(y-(10\sigma_m-1))-(y-3/7)\left(x-2\sqrt{3}\sigma_m\right)} \tag{7}$$

Using identity (5) we can express the equation of the circle with centre $\Delta^{dA}_{3m-2} = (2\sqrt{3}\sigma_m, (10\sigma_m-1))$ and radius $1/2^{3m-2}$ as: $x^2+y^2-4\sqrt{3}\sigma_m x-2\,(10\sigma_m-1)y+12\sigma_m^2+(10\sigma_m-1)^2 = 16(1-7\sigma_m)^2$.

Using this to eliminate the higher powers of x and y in the nominator of Equation (7) above and simplifying we get:

$$\frac{m_1-m_2}{1+m_1m_2} = \frac{-\sqrt{3}x-5y+51-336\sigma_m}{5x-\sqrt{3}y-\sqrt{3}}. \tag{8}$$

Taking the point B^{cA}_{3m-2} and translating it so that centre of the circle Δ^{dA}_{3m-2} of the arc on which it lies is at the origin, and rotating it through an arbitrary angle θ results in the polar coordinates $(4(1-7\sigma_m)\ \sin\ \theta, 4(1-7\sigma_m)\ \cos\ \theta)$. Translating the origin back to its original position gives $(4(1-7\sigma_m)\ \sin\ \theta+2\sqrt{3}\sigma_m, 4(1-7\sigma_m)\ \cos\ \theta+(10\sigma_m-1))$, which

is then a parameterised coordinate of an arbitrary point on the circle in question. Substituting this into Equation (8) we get:

$$\frac{m_1 - m_2}{1 + m_1 m_2} = \frac{-\sqrt{3}\sin\theta - 5\cos\theta + 14}{-\sqrt{3}\cos\theta + 5\sin\theta},$$

which is indeed independent of σ_m, $\forall 0 \leq \theta \leq 2\pi$.

The proof for the other two circles with centres Δ^{dA}_{3m-1} and Δ^{dA}_{3m} is completely analogous. The resultant arguments to the arc tan function are:

$$\frac{m_1 - m_2}{1 + m_1 m_2} = \frac{-\sqrt{3}\sin\theta + 2\cos\theta + 7}{-\sqrt{3}\cos\theta - 2\sin\theta}$$

and

$$\frac{m_1 - m_2}{1 + m_1 m_2} = \frac{-\sqrt{3}\sin\theta - 5\cos\theta + 14}{-\sqrt{3}\cos\theta + 5\sin\theta}$$

respectively, both of which are again independent of σ_m (and of m).

We have now shown that the angle the radius vector makes with the tangent to all three segments of the mth iteration are independent of σ_m and since we have already proved that the female equilateral spiral is C^1 continuous, this completes the proof. □

That the male spiral is also a geometric spiral has in fact already been proven by Theorem 2 since the point at which the lines $\bar{Y}^{dZ}_{3m+\theta}$ converge is by definition the convergence point itself.

We will now look at some nice properties of equilateral male and female spirals. To do this we first need to introduce some new notation and derive some intermediate results.

2.3. *Spiral segment intersection points*

We start by categorising all the lines $\bar{Y}^{dZ}_{n}$ which pass through the vertices of the corresponding clockwise or anti-clockwise convergence triangles. Table 8 shows the equations of these lines for the clockwise convergence triangle. For any initial vertex $Z^{d}_{\bullet}$ only six of the nine lines $\bar{Y}^{dZ}_{n}$ are distinct. These six lines can be divided into two sets of three lines each:

- One set of three lines for each vertex $Z^{d}_{\bullet}$, which we denote by $\bar{R}^{dZ}_{\Theta}$. If θ_1 and θ_2 are the tabulated orientations of the vertices corresponding to two identical lines then the orientation Θ of $\bar{R}^{dZ}_{\Theta}$ is defined set-wise by $\Theta = \{0, -1, -2\} - \{\theta_1, \theta_2\}$.
- One set of three lines for each vertex $Z^{d}_{\bullet}$, which we denote by $\bar{S}^{dZ}_{\Theta}$. The orientation Θ of $\bar{S}^{dZ}_{\Theta}$ is identical to the orientation of the line to which it corresponds.

Each spiral, be it male or female, is made up of segments joined together to form that spiral. We have seen that these segments either are, or are formed on, the side of the corresponding binated triangle which is left (anti-clockwise) for clockwise binated triangles or right (clockwise) for anti-clockwise binated triangles of the new side of that triangle. To denote these segments we introduce the notation:

$\lambda^{dZ}_{3m+\Theta}$, $\Theta = -2, -1, 0$, for the three segments of the mth male spiral iteration and
$\varphi^{dZ}_{3m+\Theta}$, $\Theta = -2, -1, 0$, for the three segments of the mth female spiral iteration.

Table 8. All the lines $\overline{Y}_n^{cZ}$.

		Initial fixed vertex		
Θ	Line	A	B	C
	$\overline{A}_{3m+\Theta}^{cZ}$	$y=\frac{\sqrt{3}}{2}x \equiv \overline{R}_{-1}^{cA}$	$y=\frac{1}{3\sqrt{3}}x+\frac{2}{3} \equiv \overline{S}_{-2}^{cB}$	$y=\frac{\sqrt{3}}{2}x-\frac{3}{4} \equiv \overline{R}_{0}^{cC}$
-2	$\overline{B}_{3m+\Theta}^{cZ}$	$y=-3\sqrt{3}x+3 \equiv \overline{R}_{0}^{cA}$	$y=-3\sqrt{3}x+6 \equiv \overline{R}_{-1}^{cB}$	$y=\frac{5}{\sqrt{3}}x-3 \equiv \overline{S}_{-2}^{cC}$
	$\overline{C}_{3m+\Theta}^{cZ}$	$y=-\frac{2}{\sqrt{3}}x+1 \equiv \overline{S}_{-2}^{cA}$	$y=-\frac{\sqrt{3}}{5}x+\frac{6}{5} \equiv \overline{R}_{0}^{cB}$	$y=-\frac{\sqrt{3}}{5}x+\frac{3}{5} \equiv \overline{R}_{-1}^{cC}$
	$\overline{A}_{3m+\Theta}^{cZ}$	$y=\frac{1}{3\sqrt{3}}x+\frac{1}{3} \equiv \overline{S}_{-1}^{cA}$	$y=\frac{\sqrt{3}}{2}x \equiv \overline{R}_{-2}^{cB}$	$y=\frac{\sqrt{3}}{2}x-\frac{3}{4} \equiv \overline{R}_{0}^{cC}$
-1	$\overline{B}_{3m+\Theta}^{cZ}$	$y=-3\sqrt{3}x+3 \equiv \overline{R}_{0}^{cA}$	$y=\frac{5}{\sqrt{3}}x-2 \equiv \overline{S}_{-1}^{cB}$	$y=-3\sqrt{3}x+6 \equiv \overline{R}_{-2}^{cC}$
	$\overline{C}_{3m+\Theta}^{cZ}$	$y=-\frac{\sqrt{3}}{5}x+\frac{3}{5} \equiv \overline{R}_{-2}^{cA}$	$y=-\frac{\sqrt{3}}{5}x+\frac{6}{5} \equiv \overline{R}_{0}^{cB}$	$y=-\frac{2}{\sqrt{3}}x+\frac{3}{2} \equiv \overline{S}_{-1}^{cC}$
	$\overline{A}_{3m+\Theta}^{cZ}$	$y=\frac{\sqrt{3}}{2}x \equiv \overline{R}_{-1}^{cA}$	$y=\frac{\sqrt{3}}{2}x \equiv \overline{R}_{-2}^{cB}$	$y=\frac{1}{3\sqrt{3}}x \equiv \overline{S}_{0}^{cC}$
0	$\overline{B}_{3m+\Theta}^{cZ}$	$y=\frac{5}{\sqrt{3}}x-1 \equiv \overline{S}_{0}^{cA}$	$y=-3\sqrt{3}x+6 \equiv \overline{R}_{-1}^{cB}$	$y=-3\sqrt{3}x+6 \equiv \overline{R}_{-2}^{cC}$
	$\overline{C}_{3m+\Theta}^{cZ}$	$y=-\frac{\sqrt{3}}{5}x+\frac{3}{5} \equiv \overline{R}_{-2}^{cA}$	$y=-\frac{2}{\sqrt{3}}x+2 \equiv \overline{S}_{0}^{cB}$	$y=-\frac{\sqrt{3}}{5}x+\frac{3}{5} \equiv \overline{R}_{-1}^{cC}$

Figure 10 shows these segments, not all of which are annotated, for a clockwise binated triangle with initial vertex A.

Each of the lines $\bar{R}_{\Theta}^{dZ}$ cuts the corresponding male segments of one complete iteration (fixed m, $\Theta=-2$, -1 and 0) of the spiral at two points. We call the intersection of $\bar{R}_{\Theta}^{dZ}$ and the segment $\lambda_{3m+\Theta}^{dZ}$, the point $\mu_{3m+\Theta}^{dZ}$, and its complement $\mu_{3m+\mathrm{mod}(\Theta-1,-3)}^{\prime dZ}$, the intersection of $\bar{R}_{\Theta}^{dZ}$ with the other segment of the mth male spiral iteration. Similarly, the intersection of $\bar{R}_{\Theta}^{dZ}$ with the segments of the mth female spiral iteration are given by the points $\eta_{3m+\Theta}^{dZ}$ and their complement $\eta_{3m+\mathrm{mod}(\Theta-1,-3)}^{\prime dZ}$ (see Figure 11 for a picture of these).

Analogously the lines $\bar{S}_{\Theta}^{dZ}$ cut the corresponding segments of the mth male spiral iteration at $\nu_{3m+\Theta}^{dZ}$ and $\nu_{3m+\mathrm{mod}(\Theta-1,-3)}^{\prime dZ}$ and the mth female spiral iteration at $\rho_{3m+\Theta}^{dZ}$ and $\rho_{3m+\mathrm{mod}(\Theta-1,-3)}^{\prime dZ}$, respectively.

We will now derive the coordinates of the eight intersection points $\mu_{3m+\Theta}^{dZ}$, $\mu_{3m+\Theta}^{\prime dZ}$, $\eta_{3m+\Theta}^{dZ}$, $\eta_{3m+\Theta}^{\prime dZ}$, $\nu_{3m+\Theta}^{dZ}$, $\nu_{3m+\Theta}^{\prime dZ}$, $\rho_{3m+\Theta}^{dZ}$ and $\rho_{3m+\Theta}^{\prime dZ}$.

We look at the intersection points defined by $\bar{R}_{-2}^{cA}$ with the male and female spiral segments (Figure 11).

From Table 8, we see that the line $\bar{R}_{-2}^{cA}$ is given by $y=-(\sqrt{3}/5)x+(3/5)$. We also know that the arc segment φ_{3m-2}^{cA} is defined by the centre $(2\sqrt{3}\sigma_m,(10\sigma_m-1))$ and radius $1/2^{3m-2}$. Solving for the x coordinate of η_{3m-2}^{cA} of the intersection of these two we get:

$$\eta_{3m-2}^{cA}(x): \quad \left(x-2\sqrt{3}\sigma_m\right)^2+\left(-\frac{\sqrt{3}}{5}x-10\sigma_m+\frac{8}{5}\right)^2=\frac{1}{2^{2(3m-2)}}$$

$$\Rightarrow 28x^2-16\sqrt{3}x+\left(2800\sigma_m^2-800\sigma_m+64-\frac{25}{2^{2(3m-2)}}\right)=0.$$

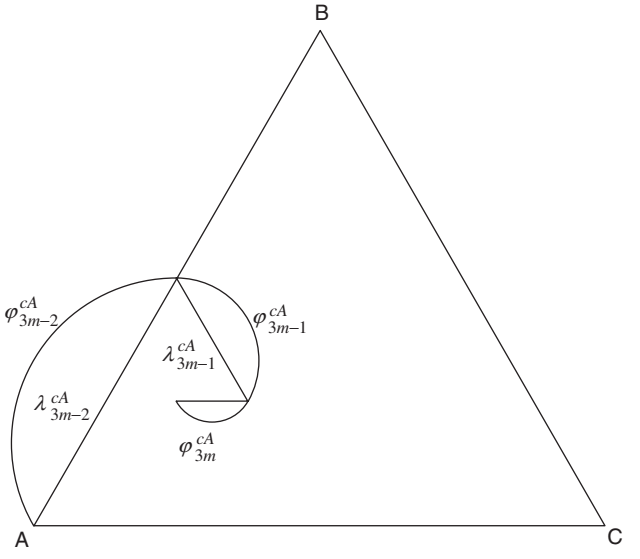

Figure 10. Annotated segments of clockwise male and female spirals for initial vertex A.

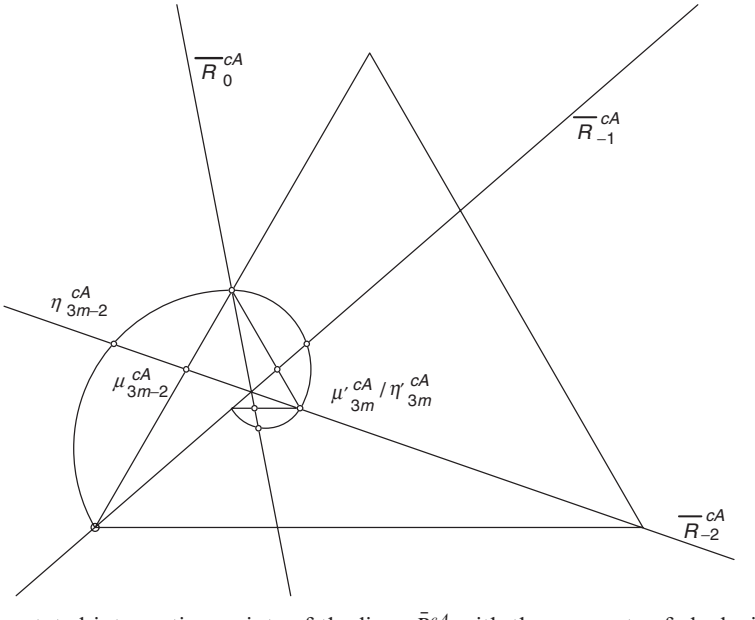

Figure 11. Annotated intersection points of the lines $\bar{R}^{cA}_{\Theta}$ with the segments of clockwise male and female spirals for initial vertex A.

Using identity (5) to eliminate the reciprocal powers of 2 from the absolute term of the above equation we have:

$$2800\sigma_m^2 - 800\sigma_m + 64 - \frac{25 \cdot 2^{10}}{2^{6(m+1)}} = 48\left(-350\sigma_m^2 + 100\sigma_m - 7\right)$$

and substituting this into the equation for the x coordinate of η_{3m-2}^{cA} above and solving for x we get:

$$\begin{aligned} &28x^2 - 16\sqrt{3}x - \frac{24}{7}\left(10 - 70\sigma_m + \sqrt{2}\right)\left(10 - 70\sigma_m - \sqrt{2}\right) = 0. \\ &\Rightarrow x = \frac{2\sqrt{3}}{7}\left(1 \pm \sqrt{1 + \frac{1}{2}\left(10 - 70\sigma_m + \sqrt{2}\right)\left(10 - 70\sigma_m - \sqrt{2}\right)}\right) \\ &= \frac{2\sqrt{3}}{7}\left(1 \pm \sqrt{\frac{1}{2}\left(2 + (10 - 70\sigma_m)^2 - 2\right)}\right) = \frac{2\sqrt{3}}{7}\left(1 \pm 5\sqrt{2}(1 - 7\sigma_m)\right) \end{aligned}$$

To determine which of these two values is the one we require, we note that $\bar{R}_{-2}^{cA}$ passes through the convergence point $(2\sqrt{3}/7, 3/7)$ and that the x coordinate of η_{3m-2}^{cA} is to the left of the convergence point. Therefore, without further ado, we can say that

$$\eta_{3m-2}^{cA}(x) = \frac{2\sqrt{3}}{7}\left(1 - 5\sqrt{2}(1 - 7\sigma_m)\right).$$

We derive the y coordinate of η_{3m-2}^{cA} by simply substituting the x coordinate in the equation for $\bar{R}_{-2}^{cA}$. We get:

$$\begin{aligned} \eta_{3m-2}^{cA}(y) &= -\frac{\sqrt{3}}{5}\frac{2\sqrt{3}}{7}\left(1 - 5\sqrt{2}(1 - 7\sigma_m)\right) + \frac{3}{5} \\ &= \frac{3}{7}\left(1 + 2\sqrt{2}(1 - 7\sigma_m)\right). \end{aligned}$$

The intersection point with the male segment λ_{3m-2}^{cA} is simpler. The λ_{3m-2}^{cA} segment is defined by the line joining the two points A_{3m-2}^{cA} and B_{3m-2}^{cA} and is given by:

$$y = \sqrt{3}x + 3(1 - 8\sigma_m).$$

Solving between this line and $\bar{R}_{-2}^{cA}$ gives:

$$\mu_{3m-2}^{cA} = \left(\frac{2}{\sqrt{3}}(10\sigma_m - 1), (1 - 4\sigma_m)\right).$$

By definition $\bar{R}_{-2}^{cA}$ passes through the points C_{3m-1}^{cA} and C_{3m}^{cA} (Figure 11), which happen to be coincident for this orientation, direction and initial vertex. Furthermore, this point also lies on both the male and female segments $\lambda_{3m-1}^{cA}/\lambda_{3m}^{cA}$ and $\varphi_{3m-1}^{cA}/\varphi_{3m}^{cA}$ respectively, thereby giving us the coordinates of $\mu_{3m}^{\prime cA}$ and $\eta_{3m}^{\prime cA}$.

The combined results after repeating the computations for $\bar{R}_{-1}^{cA}$ and $\bar{R}_{0}^{cA}$ are shown in Table 9.

The coordinates of the remaining intersection points with the lines $\bar{R}_{\Theta}^{dZ}$ with the spirals can be found in the usual way by rotation and reflection as demonstrated in Section 1.4.

The intersection points defined by $\bar{S}_{\Theta}^{cA}$ with the male and female spiral segments can be determined by an identical process.

Table 9. Coordinates of the intersection points of $\bar{R}^{cA}_{\Theta}$ and segments of the male and female spirals with initial vertex A.

$\bar{R}^{cA}_{\Theta}$	Intersection points
$\bar{R}^{cA}_{-2}$	$\eta^{cA}_{3m-2} = \left(\frac{2\sqrt{3}}{7}\left(1-5\sqrt{2}(1-7\sigma_m)\right), \frac{3}{7}\left(1+2\sqrt{2}(1-7\sigma_m)\right)\right)$
	$\mu^{cA}_{3m-2} = \left(\frac{2}{\sqrt{3}}(10\sigma_m - 1), (1-4\sigma_m)\right)$
	$\mu'^{cA}_{3m} = \eta'^{cA}_{3m} = C^{cA}_{3m-1} = C^{cA}_{3m} = \left(\sqrt{3}(1-5\sigma_m), 3\sigma_m\right)$
$\bar{R}^{cA}_{-1}$	$\eta^{cA}_{3m-1} = \left(\frac{2\sqrt{3}}{7}\left(1+2\sqrt{2}(1-7\sigma_m)\right), \frac{3}{7}\left(1+2\sqrt{2}(1-7\sigma_m)\right)\right)$
	$\mu^{cA}_{3m-1} = \left(\frac{2}{\sqrt{3}}(1-4\sigma_m), (1-4\sigma_m)\right)$
	$\mu'^{cA}_{3m-2} = \eta'^{cA}_{3m-2} = A^{cA}_{3m-2} = A^{cA}_{3(m-1)} = \left(2\sqrt{3}(8\sigma_m - 1), 3(8\sigma_m - 1)\right)$
$\bar{R}^{cA}_{0}$	$\eta^{cA}_{3m} = \left(\frac{2\sqrt{3}}{7}\left(1+\frac{\sqrt{2}}{4}(1-7\sigma_m)\right), \frac{3}{7}\left(1-\frac{3\sqrt{2}}{2}(1-7\sigma_m)\right)\right)$
	$\mu^{cA}_{3m} = \left(\frac{1}{\sqrt{3}}(1-\sigma_m), 3\sigma_m\right)$
	$\mu'^{cA}_{3m-1} = \eta'^{cA}_{3m-1} = B^{cA}_{3m-2} = B^{cA}_{3m-1} = \left(2\sqrt{3}\sigma_m, 3(1-6\sigma_m)\right)$

2.4. *Sacred geometry*

We will now look at some special properties of male and female spirals. We will look at the relative lengths of radius vectors from the corresponding centre at the convergence point to successive male and female spiral segments and the relative lengths of successive chords defined by the lines joining the successive intersection points on the spirals we have derived above. We will also show that the ratio of the radius vector and the associated chord for a particular set of intersection points are the same for both male and female spirals.

We start by defining the function $d(a, b)$ to be distance between the points a and b and for convenience define $\delta_m \equiv (1 - 7\sigma_m)$. We then define the length of the radius vector at a particular intersection point $r^{dZ}_{3m+\Theta}$ on a male or female spiral segment to be distance between this point and the corresponding convergence point for the vertex in question, $d(Z^d_{\bullet}, r^{dZ}_{3m+\Theta})$. We also define the length of the chord at $r^{dZ}_{3m+\Theta}$ to be the distance between this point and the next point inwards along the spiral of same type $\{\mu, \mu', \eta, \eta', \nu, \nu', \rho, \rho'\}$, $d(r^{dZ}_{3m+\Theta}, r^{dZ}_{3m+\Theta+1})$.

There are four groups of chords and radius vectors whose lengths we wish to compute corresponding to the lines $\bar{R}^{dZ}_{\Theta}$ and $\bar{S}^{dZ}_{\Theta}$ and their intersections with the spirals, each line cutting the spiral in two places; the lengths of the corresponding clockwise and anti-clockwise chords and radius vectors being identical. We will outline the computations only for one of these groups: $\bar{R}^{dZ}_{\Theta}$ and the corresponding intersection points $\mu^{dZ}_{3m+\Theta}$ and $\eta^{dZ}_{3m+\Theta}$ on the male and female spirals respectively. The computations for the other groups are completely analogous.

We first look at the radius vectors. For the clockwise direction c with initial vertex A we have, using Tables 6 and 9:

$$d\left(A^c_\bullet, \mu^{cA}_{3(m-1)}\right) = \frac{\sqrt{2}}{3} d\left(A^c_\bullet, \eta^{cA}_{3(m-1)}\right) = \frac{16}{\sqrt{3}\sqrt{7}}\delta_m$$

$$d\left(A^c_\bullet, \mu^{cA}_{3m-2}\right) = \frac{\sqrt{2}}{3} d\left(A^c_\bullet, \eta^{cA}_{3m-2}\right) = \frac{8}{\sqrt{3}\sqrt{7}}\delta_m$$

$$d\left(A^c_\bullet, \mu^{cA}_{3m-1}\right) = \frac{\sqrt{2}}{3} d\left(A^c_\bullet, \eta^{cA}_{3m-1}\right) = \frac{4}{\sqrt{3}\sqrt{7}}\delta_m$$

$$d\left(A^c_\bullet, \mu^{cA}_{3m}\right) = \frac{\sqrt{2}}{3} d\left(A^c_\bullet, \eta^{cA}_{3m}\right) = \frac{2}{\sqrt{3}\sqrt{7}}\delta_m$$

$$d\left(A^c_\bullet, \mu^{cA}_{3(m+1)-2}\right) = \frac{\sqrt{2}}{3} d\left(A^c_\bullet, \eta^{cA}_{3(m+1)-2}\right) = \frac{1}{\sqrt{3}\sqrt{7}}\delta_m,$$

where we have used identity (2) to transform the quantities below

$$\mu^{cA}_{3(m-1)} = \left(\frac{2}{\sqrt{3}}(1-4\sigma_m), 3(8\sigma_m - 1)\right)$$

$$\mu^{cA}_{3(m+1)-2} = \left(\frac{1}{2\sqrt{3}}(1+5\sigma_m), \frac{1}{2}(1-\sigma_m)\right)$$

$$\eta^{cA}_{3(m-1)} = \left(\frac{2\sqrt{3}}{7}(1+2\sqrt{2}(1-7\sigma_m)), \frac{3}{7}(1-12\sqrt{2}(1-7\sigma_m)\right) \text{ and}$$

$$\eta^{cA}_{3(m+1)-2} = \left(\frac{2\sqrt{3}}{7}\left(1-\frac{5\sqrt{2}}{8}(1-7\sigma_m)\right), \frac{3}{7}\left(1+\frac{\sqrt{2}}{4}(1-7\sigma_m)\right)\right).$$

Thus the ratio of the lengths of successive male radius vectors, for example the quantity

$$\frac{d\left(A^c_\bullet, \mu^{cA}_{3m-2}\right)}{d\left(A^c_\bullet, \mu^{cA}_{3(m-1)}\right)},$$

is 1/2 as is the ratio of successive female radius vectors as we move inwards along the spirals.

Similarly for the chords of the male and female spirals for a fixed direction c and initial vertex A we have:

$$d\left(\mu^{cA}_{3(m-1)}, \mu^{cA}_{3m-2}\right) = \frac{\sqrt{2}}{3} d\left(\eta^{cA}_{3(m-1)}, \eta^{cA}_{3m-2}\right) = \frac{8}{\sqrt{3}}\delta_m$$

$$d\left(\mu^{cA}_{3m-2}, \mu^{cA}_{3m-1}\right) = \frac{\sqrt{2}}{3} d\left(\eta^{cA}_{3m-2}, \eta^{cA}_{3m-1}\right) = \frac{4}{\sqrt{3}}\delta_m$$

$$d\left(\mu^{cA}_{3m-1}, \mu^{cA}_{3m}\right) = \frac{\sqrt{2}}{3} d\left(\eta^{cA}_{3m-1}, \eta^{cA}_{3m}\right) = \frac{2}{\sqrt{3}}\delta_m$$

$$d\left(\mu^{cA}_{3m}, \mu^{cA}_{3(m+1)-2}\right) = \frac{\sqrt{2}}{3} d\left(\eta^{cA}_{3m}, \eta^{cA}_{3(m+1)-2}\right) = \frac{1}{\sqrt{3}}\delta_m$$

We again see that the ratio of the lengths of successive chords for male and female spirals, for example the quantity

$$\frac{d\left(\mu^{cA}_{3m-2}, \mu^{cA}_{3m-1}\right)}{d\left(\mu^{cA}_{3(m-1)}, \mu^{cA}_{3m-2}\right)},$$

as we move inwards towards the convergence point to be 1/2.

Thus, since angles and distances are preserved under rotations and reflections, we see that, as we move inwards on either the male or female spiral, the lengths of successive radius vectors and chords both decrease by a factor 1/2 for each successive segment of the spiral.

Moreover, since $d(\mu^{cA}_{3m-2}, \mu^{cA}_{3m}) = \sqrt{2}/3\ d(\eta^{cA}_{3m-2}, \eta^{cA}_{3m}) = 2\delta_m$ and $(4/\sqrt{3})^2 = 2^2 + (2/\sqrt{3})^2$, we see that the triangles $\Delta\mu^{dZ}_{3m-2}\mu^{dZ}_{3m-1}\mu^{dZ}_{3m}$ and $\Delta\eta^{dZ}_{3m-2}\eta^{dZ}_{3m-1}\eta^{dZ}_{3m}$ are right angled triangles (Figure 12) and that the triangle $\Delta\eta^{dZ}_{3m-2}\eta^{dZ}_{3m-1}\eta^{dZ}_{3m}$ is an enlargement by a factor $3/\sqrt{2}$ of the triangle $\Delta\mu^{dZ}_{3m-2}\mu^{dZ}_{3m-1}\mu^{dZ}_{3m}$ from the convergence point $A^c_\bullet$.

Doing the same for the other scenarios results in Table 10.

From Table 10 we see in fact that the ratio of the length of any two successive features of the same nature (radius vector, chord) which belong to the same set of intersection points $\{\xi^{dZ}_{3m+\Theta}, m = 1, 2, 3, \ldots\}$, $\xi = \mu, \mu', \eta, \eta', \nu, \nu', \rho, \rho'$, as we move inwards along the male or female spiral is always 1/2.

Furthermore, for the ratio of the length of any chord taken in the inwards direction towards the convergence point with the length of the corresponding radius vector from which it originates, we have:

$$\frac{d\left(\xi^{dZ}_{3m+\Theta}, \xi^{dZ}_{3m+\Theta+1}\right)}{d\left(Z^d_\bullet, \xi^{dZ}_{3m+\Theta}\right)} = \frac{\sqrt{7}}{2}, \text{ for any } \xi = \mu, \mu', \eta, \eta', \nu, \nu', \rho, \rho'.$$

Finally, every right angled triangle formed by a set of intersection points $\{\xi^{dZ}_{3m+\Theta}, \Theta = -2, -1, 0\}$ with m fixed, is such that the angle subtended by the longer of the two sides with the hypotenuse is always 30°.

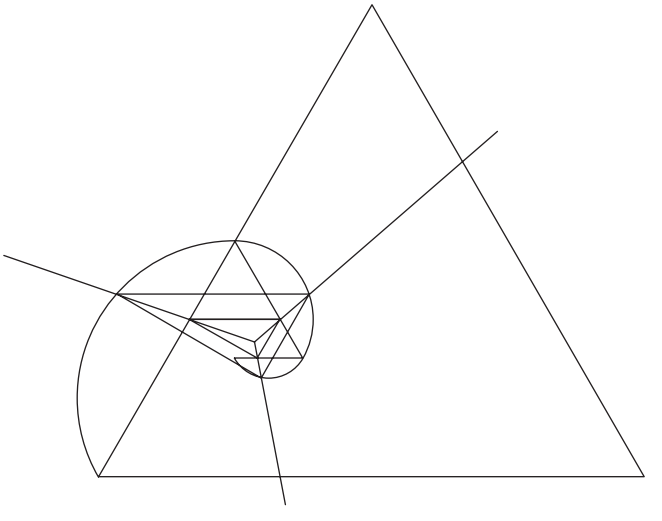

Figure 12. Right angled triangles formed by the intersection points of clockwise male and female spirals for initial vertex A.

Table 10. The sacred geometry of equilateral spirals.

Scenarios		Ratio of lengths of successive radius vectors	Ratio of lengths of successive chords	Enlargement factor right angled triangles
$\overline{R}_{\Theta}^{dZ}$	$\mu_{3m+\Theta}^{dZ}$ & $\eta_{3m+\Theta}^{dZ}$	$\frac{1}{2}$	$\frac{1}{2}$	$\frac{3}{\sqrt{2}}$
$\overline{R}_{\Theta}^{dZ}$	$\mu_{3m+\Theta}^{'dZ}$ & $\eta_{3m+\Theta}^{'dZ}$	$\frac{1}{2}$	$\frac{1}{2}$	1
$\overline{S}_{\Theta}^{dZ}$	$\nu_{3m+\Theta}^{dZ}$ & $\rho_{3m+\Theta}^{dZ}$	$\frac{1}{2}$	$\frac{1}{2}$	$\frac{5}{3}$
$\overline{S}_{\Theta}^{dZ}$	$\nu_{3m+\Theta}^{'dZ}$ & $\rho_{3m+\Theta}^{'dZ}$	$\frac{1}{2}$	$\frac{1}{2}$	2

3. Constructing equilateral spirals with ruler and compass

One way to experience sacred geometry is to construct the geometry in question using ruler and compass only. In this chapter we discuss the construction of equilateral spirals in this way.

If we start constructing male and female spirals by continuously binating triangles and each time determining the required circumcentre by constructing the intersection of the medians, then it is obvious that a lot of work is required and the result is actually neither aesthetically pleasing or accurate in the long run due to the many construction steps required. In this section we explore a number of ways to improve the construction considerably such that the end result is aesthetically pleasing, accurate and executed with a minimum of effort.

Our objective is to be able to draw both male and female spirals easily, accurately and with a minimum of lines. For a segment of a male spiral, the two end points of the line segment that define the segment are required and for the corresponding female segment the centre of the circle which defines the arc joining these same two end points is required in addition. Since segments of the male and female spirals are continuous we only need to construct two additional points to arrive at any successive male and female segment.

No measurement whatsoever is ever used in ruler and compass constructions, instead constructions have the quality of being inherently and intrinsically accurate. To retain that quality in the construction of our spirals, we further require that any two straight lines whose intersection defines either the end point of a segment or the centre of a circle, must intersect each other at right angles or very close to right angles as this gives the sharpest possible definition of the point.

3.1. *Method 1*

Given the above observations we can now proceed with our first construction method. This construction has been designed by doing the segmentation process and determining the circumcentre and then observing which lines define the required points, keeping in mind the quality we talked about above.

We will only construct three consecutive segments of each spiral. Further segments can be drawn by continuing the process. Our construction here will be based on a cycle of segments corresponding to $n = 3(m-1)$, $3m-2$ and $3m-1$, which is different to the work done in Section 2 where our proofs and derivations were time and again based on the cycle

of segments $n = 3m - 2$, $3m - 1$ and $3m$. We will call our cycle of any three consecutive segments an *iteration* of the spiral. We begin as usual with the clockwise male and female spirals for initial vertex A.

The first step is to draw the circle in which our spirals are to be constructed and to divide the circumference of this circle into six arcs of equal length in the usual way. Next we draw the three diagonals through these six points, all of which pass through the centre of the circle. This process gives us seven points (labelled 1–7 in Figure 13) from which we can define the first male and female segments: the two ends of the first segment are marked with small open circles (points 1 and 3) and the centre of the arc defining the first female segment is marked with a small closed circle (point 7). In all successive drawings we will continue to mark the ends of segments and the centres of arcs in this way. We also note in this drawing that the vertical diagonal is not in fact necessary. However, we will need this in the next step so it is convenient to draw it now.

For the second segments we need to define two additional points: one segment end (the start of the second segment is defined by the end of the first) and the centre of the circle required to draw the female arc. These two points are constructed by drawing the chords 2-4 and 3-5 as indicated in Figure 13. These chords intersect the corresponding diagonals at right angles at the points we require.

The two points for the final male and female segments require the construction of five new lines to define them. First we draw two more, in this case horizontal, chords, 1-3 and 4-6, analogous to those in step two. The intersection of these chords with the vertical diagonal in Figure 14 define required intermediate points 11 and 12. Next, the intersection of the line segments 3-11 and 4-12 defines the centre, 13, of the circle for the third arc segment; note that these lines do not quite intersect at right angles (arc tan $(3\sqrt{3}) \approx 79^\circ$) but still acceptably close. The final line 10-12 intersects the diagonal 3-6 at right angles and defines point 14, the end of the third spiral segment.

We now have constructed all the points (1, 3, 10, 14, 7, 8, 13) required to draw the first three segments of the male and female spirals by drawing one circle and 10 line segments.

Two further remarks on the construction above are worth making:

- We can draw in the corresponding convergence point. In Figure 14: (a) join the points 1-5; (b) join the point where this segment cuts the segment 4-6 with the vertex 3; (c) this segment cuts the segment 4-12 at right angles at the convergence point.
- Looking at Figure 14 we can see the right angled triangles formed by the start points of the spiral segments (1-3-10), the end points of the segments (3-10-14) and the centres of the circles defining the arcs of the female spiral iteration (7-8-13). This final right angled triangle was discussed in Section 2.2.

We could continue to define spiral segments in this way. For example, starting from Figure 14, the next male and female segments require five further lines as shown in Figure 15. However, we see that one of the line segments defining the centre of the circle for the female segment is very short, which will inevitably lead to inaccuracies in our construction. This phenomenon only gets increasingly worse as we move inwards defining new segments as we go.

Therefore, rather than proceeding in this way, we take the complete process for constructing an iteration of three arcs as shown in Figure 14 as a clockwise *unit of construction* which we then propagate repeatedly inwards along the spiral similar to a

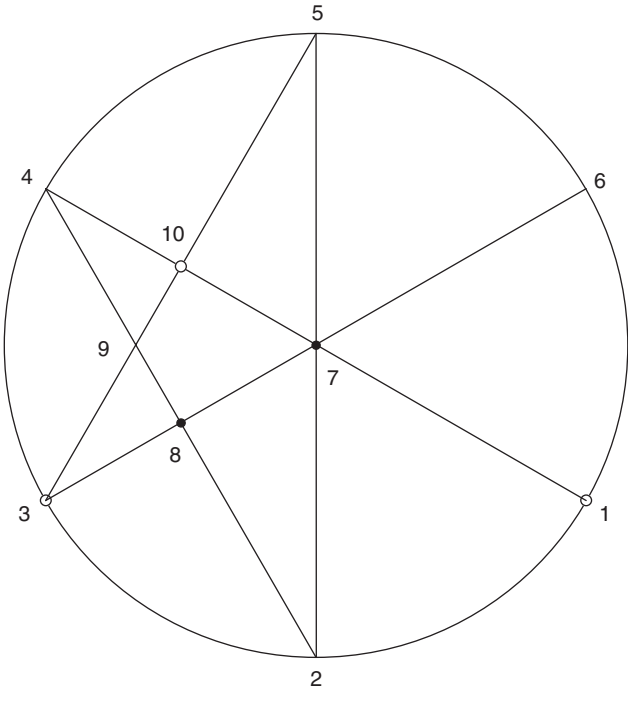

Figure 13. The points required to draw the first and second male and female segments.

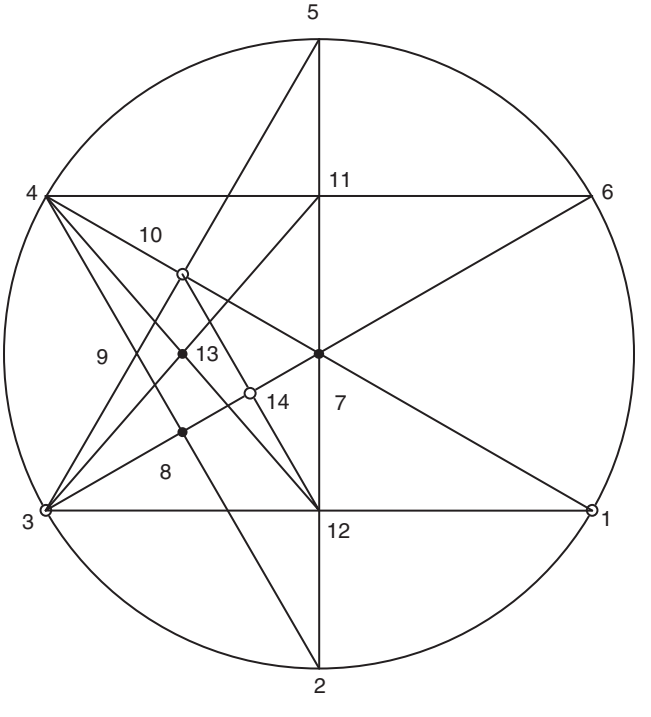

Figure 14. The additional points 13 and 14 required to draw the third male and female segments.

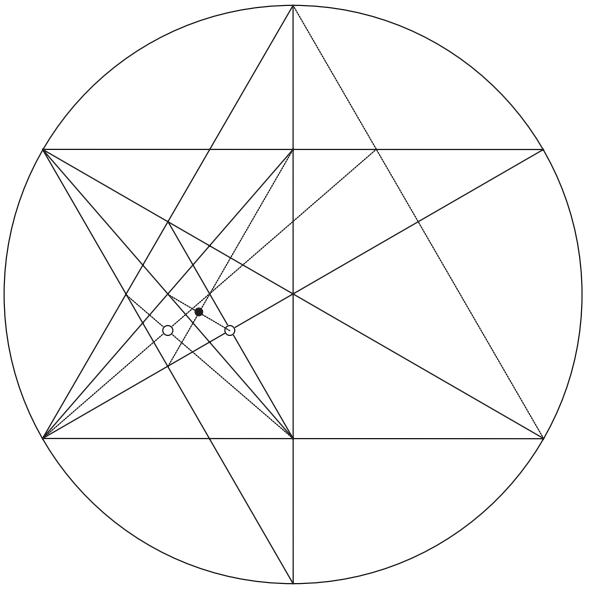

Figure 15. The additional line segments required to construct the next $n = 3m$ clockwise male and female spiral segment.

fractal construction. One further iteration of this unit of construction is shown in Figure 16 and we can see immediately that this leads to more intrinsic accuracy in the drawing.

Looking at Figure 16 we see that the centre of the second clockwise unit of construction corresponds with point 13 in Figure 14. In general we can easily show (Section 3.2) that with respect to the previous unit of construction:

- The centre of the unit of construction containing the segments $3m$, $3m+1$ and $3m+2$ is at Δ_{3m}^{dZ}. Thus, while the unit of construction contains all the construction points for three consecutive segments, each successive construction in fact only produces the points for two new male and two new female segments.
- The new unit of construction is rotated through an angle of 120° with respect to the previous one;
- The radius of the circle containing the unit of construction is 1/4 that of the previous one.

3.2. *Method 2*

By using method 1 to construct the segment start and end points and arc centres between these points we see that all of these are located on four circles. These points and the corresponding circles are shown in Figure 17.

It is interesting to compute the radii of these four circles. To do this we assume without loss of generality that our unit of construction contains an iteration of the spiral consisting of the segments $3m$, $3m+1$ and $3m+2$. Since the points for the clockwise and anti-clockwise arcs fall on the same circles, we will consider only the clockwise case. In computing the various radii, remember that the solid points are the centres of arcs (circumcircles) and the hollow points are terminating points for spiral segments (vertices of equilateral triangles).

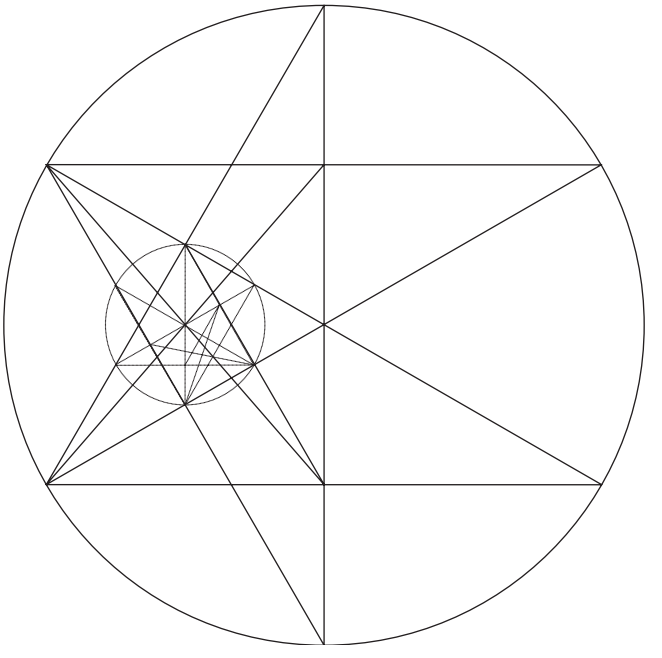

Figure 16. Segments of clockwise male and female spirals formed from two iterations of the clockwise *unit of construction*.

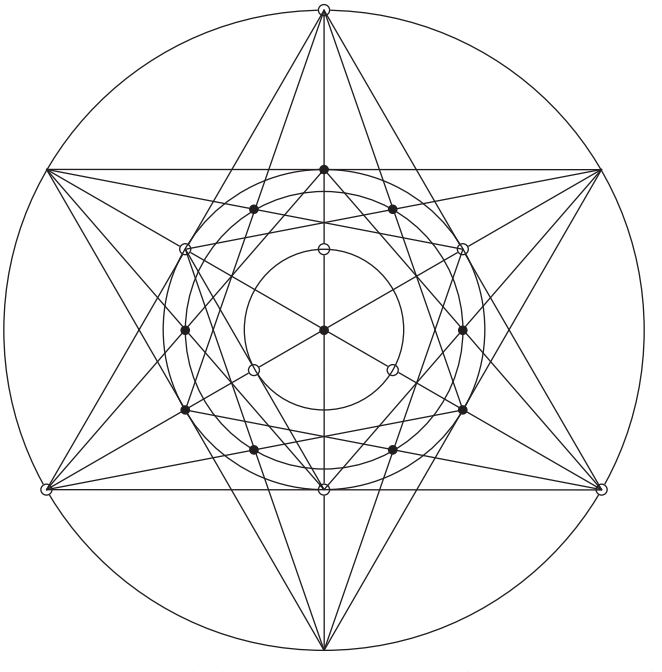

Figure 17. The four circles on which the construction points for an iteration of male and female segments lie.

From Table 7 we see that the generic centre of the four circles lies at $\Delta_{3m}^{cA} = ((\sqrt{3}/2)(1-3\sigma_m), (1/2)(1-\sigma_m))$. Using Table 2 we can now compute the radius of the outer most circle, using for example the vertex A:

$$d\left(\Delta_{3m}^{cA}, A_{3m}^{cA}\right) = \delta_m.$$

For the circle with the next biggest radius we need to compute $d(\Delta_{3m}^{cA}, \Delta_{3(m+1)-2}^{cA})$. Using the identity (2) to express the different centres in terms of σ_m, we can show that the four quantities we require in order of decreasing magnitude are:

$$\Delta_{3(m+1)-2}^{cA} = \left(2\sqrt{3}\sigma_{m+1}, 10\sigma_{m+1} - 1\right) = \left(\frac{\sqrt{3}}{4}(\sigma_m + 1), \frac{1}{4}(5\sigma_m + 1)\right) \quad \text{and}$$

$$d\left(\Delta_{3m}^{cA}, \Delta_{3(m+1)-2}^{cA}\right) = \frac{1}{2}\delta_m.$$

Similarly for the circle with the next biggest radius we need to compute $d(\Delta_{3m}^{cA}, \Delta_{3(m+1)-1}^{cA})$:

$$d\left(\Delta_{3m}^{cA}, \Delta_{3(m+1)-1}^{cA}\right) = \frac{\sqrt{3}}{4}\delta_m.$$

Finally for the inner most circle, we need to compute $d(\Delta_{3m}^{cA}, C_{3(m+1)-1}^{cA})$:

$$d\left(\Delta_{3m}^{cA}, C_{3(m+1)-1}^{cA}\right) = \frac{1}{4}\delta_m.$$

Note that for the next iteration for segments $3m+2$, $3m+3$ and $3m+4$ we will need to compute $d(\Delta_{3m}^{cA}, B_{3(m+2)-2}^{cA})$ for the inner most circle.

To construct all the points needed to complete a single iteration for our second construction method we proceed as follows (Figure 18):

Divide the circumference of the circumcircle into six equal segments in the usual way.

Sequentially label these points 1, 2, 3, 4, 5 and 6.

Draw the three diagonals 1-4, 2-5, 3-6.

Draw the six chords 1-3, 2-4, 3-5, 4-6, 5-1, 6-2.

Sequentially label the points 7, 8, 9, 10, 11, 12 where these chords intersect.

The points where the chords cut the diagonals define the points on the second outer most circle. Label these points 13, 14, 15, 16, 17, 18.

Draw the diagonals 7-10, 8-11, 9-12.

Join, for example 1-15 and 2-18.

Where these two intersect (at almost right angles) on the diagonal 7-10 defines a point on the circumference of the second inner most circle. The remaining points are given by the intersection of the diagonals 7-10, 8-11, 9-12 with the circle.

Finally draw, for example, the chord 14-18.

Where this chord intersects the diagonal 1-4 defines a point on the circumference of the inner most circle. The remaining points are given by the intersection of the diagonals 1-4, 2-5 and 3-6 with the circle.

Whether method 1 or method 2 is better is a matter of personal preference and usually defined by the application at hand. In terms of construction effort, method 1 requires 24 line segments in the outer circumcircle; method 2 requires 15 line segments and three circles.

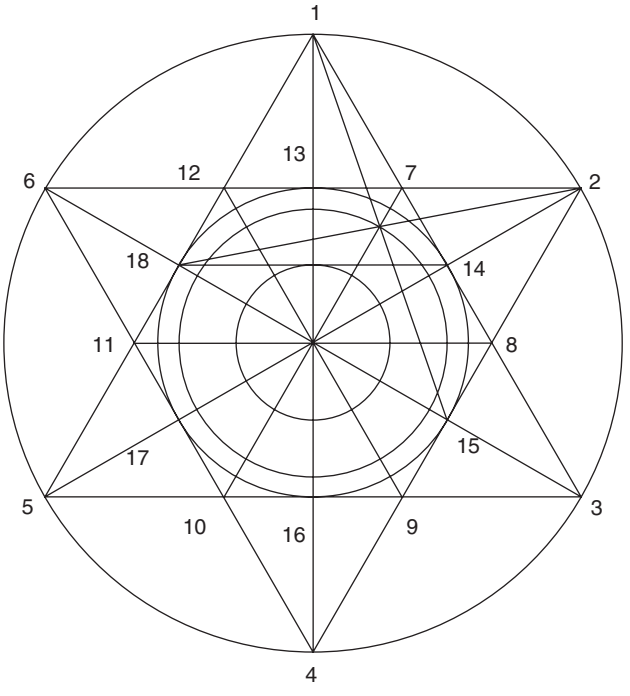

Figure 18. Using method 2 to construct the points for assembling an iteration of spirals.

Reference

[1] M.S. Schneider, *A Beginner's Guide to Constructing the Universe*, Harper Perennial, New York, 1995.